Ni(II) and Pd(II) Complexes Bearing Novel Bis(β-ketoamino) Ligand and Their Catalytic Activity toward Copolymerization of Norbornene and 5-Norbornene-2-yl Acetate Combined with $B(C_6F_5)_3$

KAITI WANG, YIWANG CHEN, XIAOHUI HE, YUEMAN LIU, WEIHUA ZHOU

Institute of Polymers, Nanchang University, 999 Xuefu Avenue, Nanchang 330031, China

Received 25 March 2011; accepted 8 May 2011
DOI: 10.1002/pola.24767
Published online 26 May 2011 in Wiley Online Library (wileyonlinelibrary.com).

ABSTRACT: Two complexes $Mt\{C_{10}H_8(O)C[N(C_6H_5)]CH_3\}_2$ [Mt = Ni(II); Mt = Pd(II)] were synthesized, and the solid-state structures of the complexes have been determined by single-crystal X-ray diffractions. Homopolymerization of norbornene (NB) and copolymerization of NB and 5-norbornene-2-yl acetate ($NB\text{-}OCOCH_3$) were carried out in toluene with both the two complexes mentioned above in combination with $B(C_6F_5)_3$. Both the catalytic systems exhibited high activity toward the homopolymerization of NB (as high as 2.7×10^5 $g_{polymer}/mol_{Ni}$ h, for Ni(II)/$B(C_6F_5)_3$ and 2.1×10^5 $g_{polymer}/mol_{Pd}$ h for Pd(II)/$B(C_6F_5)_3$, respectively.). Although the Pd(II)/$B(C_6F_5)_3$ shows very lower activity toward the copolymerization of NB with $NB\text{-}OCOCH_3$, Ni(II)/$B(C_6F_5)_3$ shows a high activity and produces the addition-type copolymer with relatively high molecular weights (MWs; 1.80–2.79 $\times 10^5$ g/mol) as well as narrow MW distribution (1.89–2.30). The $NB\text{-}OCOCH_3$ content in the copolymers can be controlled up to 5.8–12.0% by varying the comonomer feed ratios from 10 to 50%. The copolymers exhibited high transparency, high glass transition temperature ($T_g > 263.9$ °C), better solubility, and mechanical properties compared with the homopolymer of NB. The reactivity ratios of the two monomers were determined to be $r_{NB\text{-}OCOMe} = 0.08$, $r_{NB} = 7.94$ for Ni(II)/$B(C_6F_5)_3$ system, and $r_{NB\text{-}OCOMe} = 0.07$, $r_{NB} = 6.49$, for Pd(II)/$B(C_6F_5)_3$ system by the Kelen-Tüdõs method. © 2011 Wiley Periodicals, Inc. J Polym Sci Part A: Polym Chem 49: 3304–3313, 2011

KEYWORDS: additional polymerization; late-transition-metal catalyst; norbornene; olefin polymerization catalyst; organometallic catalysis; polymer synthesis; reactivity ratio

INTRODUCTION Norbornene (NB; bicycle[2.2.1]hept-2-ene) is polymerized by cationic or radical polymerization,[1–3] ring-opening metathesis polymerization,[4–11] and vinyl-type addition polymerization.[12–21] The increasing interest in vinyl-type polynorbornene (PNB) is due to its high glass transition temperature, high optical transparency, low dielectric constant, and low birefringence. However, it shows poor processability and poor solubility. To modify the disadvantages and get functionalized PNB, a series of copolymers of NB with ethylene,[22–28] propylene,[29–31] higher 1-alkene,[32] polar monomer,[33–35] and NB derivatives[36–40] have been also studied.

Shiono et al.[32] prepared the copolymer of NB with 1-hexene, 1-octene, and 1-decene. The 1-alkene content of the copolymers is 7.0–58.0%, and the copolymer can be dissolved in common organic solvents. The copolymer films obtained from CH_2Cl_2 exhibited high transparence. Mi et al.[34] got the copolymers of NB and styrene by Pd- and Ni-based novel bridged dinuclear diimine complexes and methylaluminoxane (MAO). The reactivity ratios were $r_{styrene} = 0.281$ and $r_{NB} = 18.7$. The styrene incorporated are 0.6–46.5 mol %, and the packing density, thermostability, and the glass transition temperatures of copolymers are increased relative to polystyrene. The solubility and processability of the copolymers are improved relative to PNB. Kaita et al.[36] used cyclopentadienyl nickel and palladium complexes catalyzed the copolymerization of NB with NB carboxylic acid esters. The copolymers of NB with 5-norbornene-2-carboxylic acid methyl ester has high molecular weights (MWs; M_n = 234,100–109,500), narrow MW distributions ($M_w/M_n = 1.78$–1.89), and high glass transition temperature (352.8–316.0 °C). The content of 5-norbornene-2-carboxylic acid methyl ester in the copolymers is 17.4–60.7%, and the copolymer can be dissolved in common organic solvents.

The vinyl-type PNB can be obtained through Ziegler-Natta,[22–25,30–32] metallocene,[12,29] rare earth metal,[26,33,41] and late transition metal catalysts.[13–21,27,28,34–40,42–47] The late transition metal catalysts are simple to synthesize and show more stable to polar NB detectives. The common late transition metal catalysts are Ni(II) and Pd(II) complexes. The complexes usually contain O, O—, O, N—, N, N— donor, and phosphines ligand. The solubility of PNB catalyzed by Ni(II) complexes are better than those catalyzed by Pd(II) complexes.

Additional Supporting Information may be found in the online version of this article. Correspondence to: X. He (E-mail: hexiaohuishulei@yahoo.com.cn) or Y. Chen (E-mail: ywchen@ncu.edu.cn)

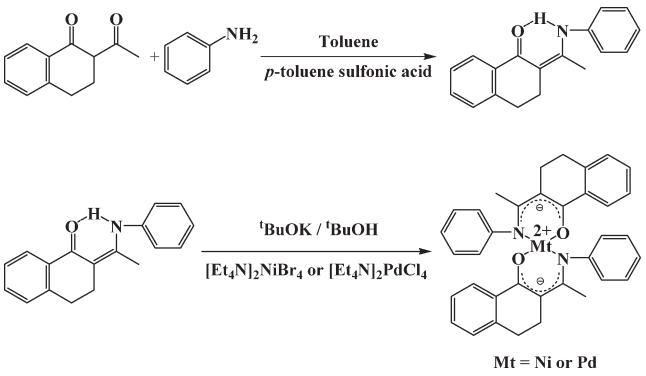

SCHEME 1 The synthetic route of the complexes.

In last decade, some β-ketoamino catalysts[39,40,42,43] have been synthesized and exhibited excellent activity on polymerization of NB, and there is a phenomenon that the electron-drawing group (such as $-CF_3$, $-C_6H_5$) can increase the activity of the complexes. The polymerization usually requires both organometallics complexes and cocatalyst. MAO, modified MAO (MMAO), or $B(C_6F_5)_3$ were often chosen as cocatalyst. In this article, the copolymerization behavior of NB and 5-norbornene-2-yl acetate (NB-$OCOCH_3$) catalyzed by two Ni(II) and Pd(II) catalysts bearing novel β-ketoamino combined with $B(C_6F_5)_3$ cocatalyst was reported, the new ligand, which contains benzocyclohexan ring on 2-acetyl-1-tetralone and phenyl ring on aniline, which show a big steric effect and strong electronic effect, the conjugation effect of phenyl and benzocyclohexan rings also enhances the electronic effect, so the two new catalysts would show better stability and higher catalytic activity. The thermal, optical, and mechanical properties of the copolymer were also shown in this article.

EXPERIMENTAL

Materials

All the reactions were performed under an atmosphere of dry and oxygen-free argon using standard vacuum, Schlenk, or under nitrogen atmosphere in glove box (MBraun). Toluene was refluxed and distilled from sodium and benzophenone under dry nitrogen. NB was purchased from Alfa Aesar and purified through drying by sodium and distilled under dry nitrogen, then made a solution (4.25 mol/L) in toluene.

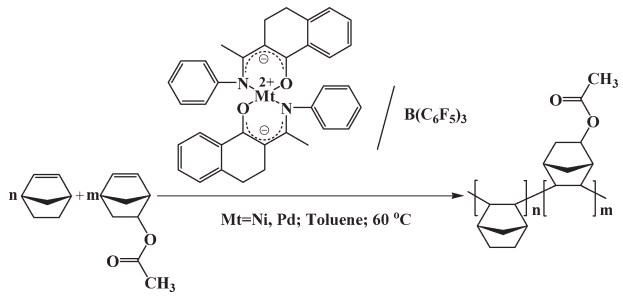

SCHEME 2 Copolymerization of norbornene and 5-norbornene-2-yl acetate catalyzed by Ni(II) and Pd(II) complexes.

5-Norbornene-2-yl acetate was purchased from Aldrich and purified by anhydrous Magnesium Sulfate. Other commercially available reagents were purchased and used without purification.

Characterization

The intensity data of the single crystals were collected on the CCD-Bruker Smart APEX II system. The element analysis was performed on elementar-vario EL cube elemental analyzer. The nuclear magnetic resonance (NMR) of the polymers was recorded on a Bruker ARX 600 NMR spectrometer at ambient temperature, with $CDCl_3$ as the solvent. The XT4A melting point measure instrument (BeiJing KeYi electro-optic instrument factory, China) was used to test the melting point temperature. The gel permeation chromatography (GPC) was conducted with a Breeze Waters system equipped with a Rheodyne injector, a 1515 Isocratic pump, and a Waters 2414 differential refractometer using polystyrenes as the standard and chloroform ($CHCl_3$) as the eluent at a flow rate of 1.0 mL/min and 40 °C through a Styragel column set, Styragel HT3, and HT4 (19×300 mm^2, $10^3 + 10^4$ Å) to separate MW ranging from 10^2 to 10^6. The IR spectra were recorded by a Shimadzu IR Prestige-21 FTIR spectrophotometer. The wide-angle X-ray diffraction (WXRD) curves were recorded on a Bruker D8 Focus X-ray diffractometer, operating at 40 kV and 40 mA with a copper target (λ = 1.54 Å) and at a scanning rate of 2°/min. The thermal gravimetric analysis (TGA) measurements were performed on a Perkin-Elmer instrument TGA 7 from room temperature to 600 °C at a rate of 20 °C/min under nitrogen atmosphere. The differential scanning calorimetry (DSC) measurements were obtained on a Shimadzu DSC-60 with a heating/cooling rate of 10 °C/min under nitrogen atmosphere. The dynamic thermomechanical analysis (DMA) was performed on a TA

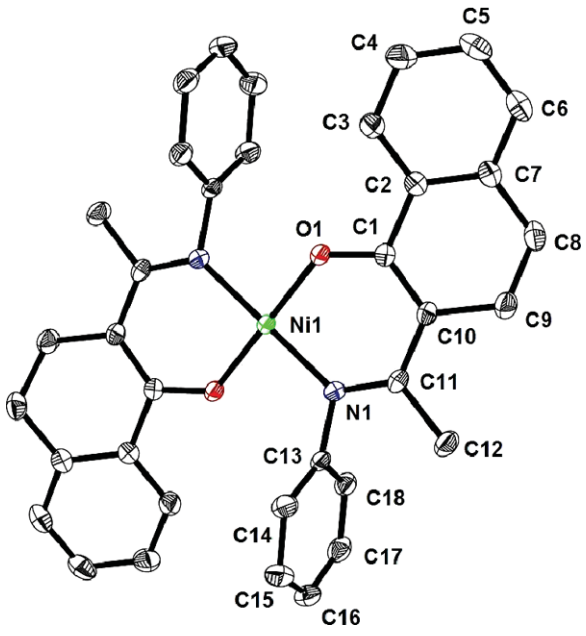

FIGURE 1 ORTEP plots of Ni(II) complex showing the atom-labeling scheme. Hydrogen atoms are omitted for clarity.

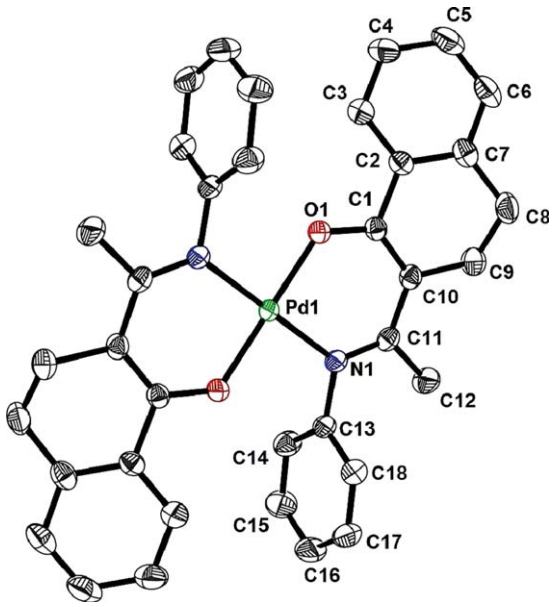

FIGURE 2 ORTEP plots of Pd(II) complex showing the atom-labeling scheme. Hydrogen atoms are omitted for clarity. [Color figure can be viewed in the online issue, which is available at wileyonlinelibrary.com.]

Q800 DMA at a heating rate of 3 °C/min and a frequency of 1 Hz. The UV–vis spectra were recorded on a Hitachi UV-2300 spectrophotometer. The mechanical properties were measured on a CMT8502 Machine model GD203A (ShenZhen Sans Testing Machine, China) at a speed of 5 mm/min.

Ligands and Complexes Syntheses

The complexes bearing bis-(β-ketoamino) ligands Mt{$C_{10}H_8$(O)C[N(C_6H_5)]CH_3}$_2$ [Mt = Ni(II), Mt = Pd(II)], were synthesized according to the method reported in our previous work.[42] The synthetic route was shown in Scheme 1.

{$C_{10}H_8$(O)C[HN(C_6H_5)]CH_3}

2-Acetyl-1-tetralone (4.71 g, 0.025 mol), aniline (2.28 mL, 0.025 mol), and a catalytic amount of *p*-toluenesulfonic acid in toluene (150 mL) were combined and refluxed for 3 h. Water was removed as a toluene azeotrope at 125–130 °C using a water separator. Volatile was removed *in vacuo* and yellow crystals of {$C_{10}H_8$(O)C[HN(C_6H_5)]CH_3} was obtained by recrystallization from *n*-hexane.

Yield: 64.7%, Mp: 117 °C. ^{1}H NMR ($CDCl_3$), δ (ppm): 14.12 (s, 1H, O···H—N); 7.31–8.04 (m, 4H, $C_{10}H_8$); 6.74–7.25 (m, 5H, C_6H_5); 2.61–2.90 (m, 4H, $C_{10}H_8$); 2.14 (s, 3H, CH_3). ^{13}C NMR ($CDCl_3$), δ (ppm): 16.61 (s, 1C, RCH_3); 24.85 (s, 1C, RCH_2R); 29.11 (s, 1C, RCH_2R); 102.79 (s, 2C, C_6H_5); 125.12 (s, 1C, C_6H_5); 125.39 (s, 1C, $C_{10}H_8$); 126.50 (s, 1C, $C_{10}H_8$); 126.64 (s, 1C, $C_{10}H_8$); 127.18 (s, 1C, $C_{10}H_8$); 129.18 (s, 1C, $C_{10}H_8$); 130.95 (s, 2C, C_6H_5); 135.66 (s, 1C, R_2C=R); 139.15 (s, 1C, $C_{10}H_8$); 141.28 (s, 1C, NC=R); 159.77 (s, 1C, N—C_6H_5); 184.77 (s, 1C, R_2C=O).

Ni{$C_{10}H_8$(O)C[N(C_6H_5)]CH_3}$_2$

Potassium (0.4g, 0.01mol) was dissolved in 25 mL of dried *t*-BuOH. After the potassium had dissolved, the solution was heated to 50 °C and of {$C_{10}H_8$(O)C[HN(C_6H_5)]CH_3 (1.27 g, 0.005 mol) was added. The solution changed to red brown as {$C_{10}H_8$(O)C[HN(C_6H_5)]CH_3} completely reacted with *t*-BuOK. The reaction mixture was stirred for another 20 min. The solution was then slowly cooled down to environmental temperature, and [Et_4N]$_2$NiBr$_4$ (1.87 g, 0.003mol) was introduced, the reacting mixture immediately formed a dark-green precipitate. After stirring vigorously for several hours at room temperature, the excess *t*-BuOH was removed *in vacuo*. The reacting slurry was extracted successively with hot toluene, and the mixture was filtrated quickly. The filtrate was allowed to crystallize by cooling slowly overnight. The product was isolated and dried under reduced pressure. Additional recrystallization from *n*-hexane/toluene mixture solution gave blocks of dark-green crystals.

Yield: 43.2%, ^{1}H NMR ($CDCl_3$), δ (ppm): 7.30–8.03 (m, 8H, $C_{10}H_8$); 6.23–7.06 (m, 10H, C_6H_5); 2.41–2.64 (m, 8H, $C_{10}H_8$); 1.62 (s, 6H, CH_3). ^{13}C NMR ($CDCl_3$), δ (ppm): 21.11 (s, 2C,

TABLE 1 Crystallographic Data for Ni(II) and Pd(II) Complexes

	Ni(II) Complex	Pd(II) Complex
Empirical formula	$C_{36}H_{32}N_2O_2Ni$	$C_{36}H_{32}N_2O_2Pd$
Fw (g/mol)	583.35	631.04
Crystal color	Green	Yellow
Crystal system	Monoclinic	Monoclinic
Space group	P2(1)/c	P2(1)/c
a (Å)	13.231(2)	13.345(2)
b (Å)	11.092(2)	11.178(2)
c (Å)	9.5054(17)	9.4960(17)
α (deg)	90.00	90.00
β (deg)	100.895(2)	101.032(2)
γ (deg)	90.00	90.00
V (Å^3)	1369.8(4)	1390.3(4)
Z	2	2
D_c (Mg/m^3)	1.414	1.507
Absorption coefficient (mm^{-1})	0.746	0.705
F(000)	612	648
Crystal size (mm)	0.25 × 0.12 × 0.06	0.15 × 0.15 × 0.16
θ_{max} (deg)	25.50	25.10
Index ranges	$-16 \le h \le 16$	$-15 \le h \le 15$
	$-13 \le k \le 12$	$-13 \le k \le 13$
	$-11 \le l \le 11$	$-9 \le l \le 11$
No. of params.	188	189
Goodness-of-fit on *S* (F^2)[a]	1.322	1.074
Final R indices [$I > 2\sigma(I)$]	0.0337; 0.0712	0.0186; 0.0499
R indices (all data)	0.0521; 0.0765	0.0248; 0.0546
Largest diff peak and hole (e/Å^3)	0.315 and −0.231	0.256 and −0.267

$R = \sum||F_o|-|F_c||\sum|F_o|$; $R_w = [\sum_w (F_o^2-F_c^2)^2/\sum_w (F_o^2)^2]^{1/2}$

TABLE 2 Selected Bond Lengths (Å) and Angles (deg) for Ni(II) and Pd(II) Complexes

Ni(II) Complex		Pd(II) Complex	
Bond	Length	Bond	Length
Ni(1)—O(1)	1.8338 (13)	Pd(1)—O(1)	1.9721 (14)
Ni(1)—O(1)#1	1.8338 (13)	Pd(1)—O(1)#1	1.9721 (14)
Ni(1)—N(1)	1.9170 (17)	Pd(1)—N(1)	2.0216 (15)
Ni(1)—N(1)#1	1.9170 (17)	Pd(1)—N(1)#1	2.0216 (15)
C(1)—O(1)	1.299 (32)	C(1)—O(1)	1.296 (2)
C(1)—C(10)	1.376 (3)	C(1)—C(10)	1.385 (3)
C(1)—C(2)	1.492 (3)	C(1)—C(2)	1.490 (3)
C(7)—C(8)	1.501 (3)	C(7)—C(8)	1.486 (3)
C(8)—C(9)	1.510 (3)	C(8)—C(9)	1.502 (3)
C(9)—C(10)	1.523 (3)	C(9)—C(10)	1.526 (3)
C(10)—C(11)	1.422 (3)	C(10)—C(11)	1.429 (3)
C(11)—N(1)	1.324 (3)	C(11)—N(1)	1.322 (2)
C(11)—C(12)	1.523 (3)	C(11)—C(12)	1.519 (3)
C(13)—N(1)	1.448 (3)	C(13)—N(1)	1.442 (2)
Bond	Angle	Bond	Angle
O(1)—Ni(1)—O(1)#1	180.00 (2)	O(1)—Pd(1)—O(1)#1	180.000
O(1)—Ni(1)—N(1)	91.67 (6)	O(1)—Pd(1)—N(1)	90.64 (6)
O(1)#1—Ni(1)—N(1)	88.33 (6)	O(1)#1—Pd(1)—N(1)	89.36 (6)
O(1)—Ni(1)—N(1)#1	88.33 (6)	O(1)—Pd(1)—N(1)#1	89.36 (6)
O(1)#1—Ni(1)—N(1)#1	91.67 (6)	O(1)#1—Pd(1)—N(1)#1	90.64 (6)
N(1)—Ni(1)—N(1)#1	180.000	N(1)—Pd(1)—N(1)#1	180.000 (1)
C(11)—N(1)—Ni(1)	126.94 (13)	C(11)—N(1)—Pd(1)	125.99 (13)
C(13)—N(1)—Ni(1)	118.91 (13)	C(13)—N(1)—Pd(1)	117.30 (12)
C(1)—O(1)—Ni(1)	129.99 (13)	C(1)—O(1)—Pd(1)	127.25 (12)
O(1)—C(1)—C(10)	125.44 (19)	O(1)—C(1)—C(10)	126.94 (18)
O(1)—C(1)—C(2)	114.84 (18)	O(1)—C(1)—C(2)	113.28 (16)
C(10)—C(1)—C(2)	119.70 (19)	C(10)—C(1)—C(2)	119.77 (17)
C(7)—C(8)—C(9)	111.7 (2)	C(7)—C(8)—C(9)	112.42 (18)
C(8)—C(9)—C(10)	112.57 (19)	C(8)—C(9)—C(10)	113.44 (18)
C(1)—C(10)—C(11)	121.24 (19)	C(1)—C(10)—C(11)	123.68 (17)
C(1)—C(10)—C(9)	118.71 (18)	C(1)—C(10)—C(9)	117.87 (18)
C(11)—C(10)—C(9)	119.95 (19)	C(11)—C(10)—C(9)	118.38 (17)
N(1)—C(11)—C(10)	123.84 (19)	N(1)—C(11)—C(10)	124.66 (17)
N(1)—C(11)—C(12)	119.84 (18)	N(1)—C(11)—C(12)	118.54 (17)
C(10)—C(11)—C(12)	116.33 (19)	C(10)—C(11)—C(12)	116.80 (17)
C(14)—C(13)—C(18)	119.7 (2)	C(14)—C(13)—C(18)	119.74 (19)
C(14)—C(13)—N(1)	120.76 (19)	C(14)—C(13)—N(1)	120.51 (18)
C(18)—C(13)—N(1)	119.36 (19)	C(18)—C(13)—N(1)	119.71 (18)
C(11)—N(1)—C(13)	114.15 (17)	C(11)—N(1)—C(13)	116.72 (15)

RCH_3); 25.03 (s, 2C, RCH_2R); 28.98 (s, 2C, RCH_2R); 104.80 (s, 4C, C_6H_5); 125.65 (s, 2C, C_6H_5); 125.75 (s, 2C, $C_{10}H_8$); 125.76 (s, 2C, $C_{10}H_8$); 125.85 (s, 2C, $C_{10}H_8$); 127.58 (s, 2C, $C_{10}H_8$); 128.23 (s, 2C, $C_{10}H_8$); 128.53 (s, 4C, C_6H_5); 129.19 (s, 2C, $R_2C{=}R$); 131.52 (s, 2C, $C_{10}H_8$); 133. 05 (s, 2C, NC=R); 149.25 (s, 2C, N—C_6H_5); 165.07 (s, 2C, $R_2C{=}O$). Anal. Tested for: C, 74.17; H, 5.48; N, 4.82. Anal. Calcd for: $C_{36}H_{32}O_2N_2Ni$: C, 74.12; H, 5.53; N, 4.80.

Pd{$C_{10}H_8$(O)C[N(C_6H_5)]CH_3}$_2$

The Pd complex was synthesized followed with the route of Ni(II) complex. $[Et_4N]_2PdCl_4$ was introduced instead of $[Et_4N]_2NiBr_4$, and yellow crystals were obtained.

Yield: 41.5%, ^{1}H NMR ($CDCl_3$), δ (ppm): 7.32–8.03 (m, 4H, $C_{10}H_8$); 6.16–7.15 (m, 5H, C_6H_5); 2.46–2.70 (m, 4H, $C_{10}H_8$); 1.73 (s, 3H, CH_3). ^{13}C NMR ($CDCl_3$), δ (ppm): 21.42 (s, 2C,

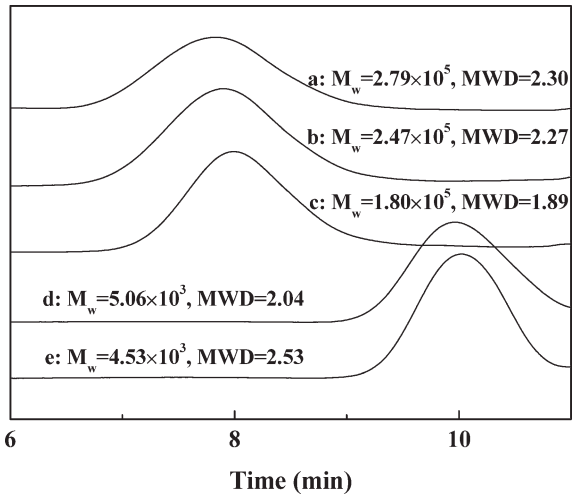

FIGURE 3 GPC curves of NB/NB-$OCOCH_3$ copolymers with: (a) 5.8%, (b) 10.3%, (c) 12.0%, (d) 3.5%, and (e) 3.7% of NBE-$OCOCH_3$ molar ratio. a, b, and c are obtained by Ni(II)/$B(C_6F_5)_3$. d and e are obtained by Pd(II)/$B(C_6F_5)_3$.

RCH_3); 26.67 (s, 2C, RCH_2R); 28.99 (s, 2C, RCH_2R); 105.35 (s, 4C, C_6H_5); 124.02 (s, 2C, C_6H_5); 124.86 (s, 2C, $C_{10}H_8$); 125.59 (s, 2C, $C_{10}H_8$); 125.61 (s, 2C, $C_{10}H_8$); 126.08 (s, 2C, $C_{10}H_8$); 126.68 (s, 2C, $C_{10}H_8$); 127.72 (s, 4C, C_6H_5); 128.77 (s, 2C, R_2C=R); 128.89 (s, 2C, $C_{10}H_8$); 134.25 (s, 2C, NC=R); 149.36 (s, 2C, N—C_6H_5); 165.53 (s, 2C, R_2C=O). Anal. Tested for: C, 68.46; H, 5.20; N, 4.53. Anal. Calcd for $C_{36}H_{32}O_2N_2Pd$: C, 68.52; H, 5.11; N, 4.44.

Polymerization

All procedures were carried out under purified nitrogen atmosphere. A typical copolymerization procedure is as follow: a toluene solution of NB and 5-norbornene-2-yl acetate was added via a syringe into a 100-mL two-necked round-bottomed flask containing a magnetic stirrer, the complexes solution was then introduced followed by $B(C_6F_5)_3$ solution. The total volume was kept constant at 10 mL. The polymerization was performed at 60 °C for 30 min. The polymerization was quenched by ethanol/HCl (v/v = 9/1) solution and stayed overnight. The polymers were then obtained through filtration or centrifugation and washed by ethanol several times and were dried at 40 °C for 24 h in a vacuum oven. The *o*-dichlorobenzene solutions of different copolymers were used to prepare the copolymer films on glass slides. The transparent films that were obtained had thickness of about 40 μm. The copolymerization procedure and the structure of the catalysts are shown in Scheme 2.

RESULTS AND DISCUSSION

The Structures of the Two Complexes

The molecular structures of the two complexes were determined by single crystal X-ray diffraction. Single crystal of complexes suitable for X-ray diffraction study was grown from a concentrated toluene solution at room temperature. The ORTEP plots are shown in Figures 1 and 2. The crystallographic data are summarized in Table 1. CIF data of Ni$\{C_{10}H_8(O)C[N(C_6H_5)]CH_3\}_2$ and Pd$\{C_{10}H_8(O)C[N(C_6H_5)]CH_3\}_2$ complexes are available as Supporting Information. Table 2 lists the selected bond lengths and angles. The coordination geometries of the two complexes were demonstrated to be very similar in the solid state. They are both mononuclear and four coordinate. The center metal ion in the complexes and the N,O-chelator create two stable six-member chelate rings. The angle of N—Mt—N and O—Mt—O are 180.0°, the N—Mt—O angles are slightly more than 90° (N—Ni—O is 91.67(6), N—Pd—O is 90.64(6)), the N—Mt—O#1 angles are slightly less than 90° (N—Ni—O#1 is 88.33(6), N—Pd—O#1

TABLE 3 Copolymerization of Norbornene (NB) and 5-Norbornene-2-yl Acetate (NB-$OCOCH_3$) Catalyzed by Ni(II) or Pd(II) Complex Combined with $B(C_6F_5)_3$

Entry	[Mt]	NB/NB-$OCOCH_3$ (mol/mol)	Yield (%)	Activity ($g_{polymer}/mol_{Mt}$ h)	M_w (g/mol)[a]	M_n/M_w[a]	Mol % of NB-$OCOCH_3$ in Copolymers[b]	T_g[c] (°C)
1	Ni	100/0	71.1	2.7×10^5	Insoluble	–	0	302.4
2	Ni	90/10	56.8	2.3×10^5	2.79×10^5	2.30	5.8	277.5
3	Ni	70/30	33.9	1.5×10^5	2.47×10^5	2.27	10.3	274.6
4	Ni	50/50	14.4	7.1×10^4	1.80×10^5	1.89	12.0	263.9
5	Ni	0/100	Trace	–[d]	–	–	–	–
6	Pd	100/0	54.4	2.1×10^5	Insoluble	–	0	275.0
7	Pd	90/10	4.9	2.0×10^4	5.06×10^3	2.04	3.5	268.3
8	Pd	70/30	0.9	4.2×10^3	4.53×10^3	2.53	3.7	243.2
9	Pd	50/50	Trace	–	–	–	–	–
10	Pd	0/100	Trace	–	–	–	–	–

Conditions: n[complex] is 5.0×10^{-6} mol, cocatalyst is $B(C_6F_5)_3$, B/complex/monomer (n/n/n) is 20/1/2000, polymerization temperature is 60 °C, polymerization time is 30 min, the solvent is toluene, the total volume is 10 mL.

[a] Determined by GPC versus polystyrene standards in $CHCl_3$.
[b] Determined by ^1H NMR spectroscopy in $CDCl_3$.
[c] Determined by DSC analysis.
[d] Not determined.

TABLE 4 Copolymerization of NB and NB-$OCOCH_3$ Catalyzed by Ni(II) or Pd(II) Complex Combined with $B(C_6F_5)_3$

Entry	[Mt]	The Amount of Mt (10^{-6} mol)	NB/NB-$OCOCH_3$ (mol/mol)	Time (h)	Yield (%)	Mol % of NB-$OCOCH_3$ in Copolymer[a]
1	Ni	0.5	60/40	0.33	5.32	7.39
2	Ni	0.5	50/50	0.42	5.51	9.04
3	Ni	0.5	40/60	2	1.48	12.80
4	Ni	0.5	30/70	12	2.05	20.45
5	Ni	0.5	20/80	12	0.75	22.70
6	Pd	1	90/10	12	4.71	1.61
7	Pd	1	80/20	12	4.71	1.93
8	Pd	1	70/30	12	3.39	4.03
9	Pd	1	60/40	12	1.81	8.05
10	Pd	1	50/50	12	0.76	9.25

[a] Determined by ^1H NMR spectroscopy in $CDCl_3$.

is 89.36(6)). The N—Ni length is 1.9170(17), O—Ni length is 1.8338(13) in Ni(II) complex, N—Pd length is 2.0216(15), O—Pd length is 1.9721(14) in Pd(II) complex.

Copolymerization of NB and NB-$OCOCH_3$

All the experiments were carried out with Ni(II) or Pd(II) complex in the presence of $B(C_6F_5)_3$ in toluene at 60 °C for 30 min under nitrogen atmosphere. Both of complexes, activated with $B(C_6F_5)_3$, exhibit high catalytic activity for the vinyl-type addition homopolymerization of NB and Ni(II)/$B(C_6F_5)_3$ exhibit high catalytic activity on copolymerization of NB and NB-$OCOCH_3$. The activity of homopolymerization of NB catalyzed by Ni(II)/$B(C_6F_5)_3$ is up to 2.7×10^5 $g_{polymer}/mol_{Ni}$ h. The obtained PNB show good solubility in both of *o*-dichlorobenzene and cyclohexane, while the PNB obtained by Pd(II)/$B(C_6F_5)_3$ can only be dissolved in *o*-dichlorobenzene. The copolymers of NB and NB-$OCOCH_3$, however, are soluble in common organic solvents (such as $CHCl_3$, CH_2Cl_2, cyclohexane) as well as *o*-dichlorobenzene.

The obtained copolymers were characterized by GPC and shown in Figure 3. The M_w of the copolymers obtained by Ni(II)/$B(C_6F_5)_3$ are all up to 10^5, the M_w of the polymers obtained by Pd(II)/$B(C_6F_5)_3$ are as low as $5.06–4.53 \times 10^3$, and WMD of the obtained polymers are all relative narrow (WMD = 1.89–2.53).

The MWDs are relative narrow and appear as a single modal in the GPC chromatogram, which indicate copolymerization occurs at the single active site, and the products are the true copolymers instead of blends of the homopolymers, and the results of polymerizations are presented in Table 3.

Polymer yields and catalytic activities depended on the reaction conditions. As shown in Table 3, the catalytic activities of Ni(II)/$B(C_6F_5)_3$ are higher than that of Pd (II)/$B(C_6F_5)_3$, and the catalytic activities of the complexes decrease with the content of NB-$OCOCH_3$ increasing in the comonomer feed ratio. But, the Pd (II)/$B(C_6F_5)_3$ complex shows lower activity on the copolymerization of NB and NB-$OCOCH_3$. Almost no homopolymer of NB-$OCOCH_3$ were obtained by both of complexes. This is common for functionalized NB detectives, which oxygen atom competing with the double-bond for the coordination. High concentration of oxygen atom will impede double-bond coordination. When NB and NB-$OCOCH_3$ were

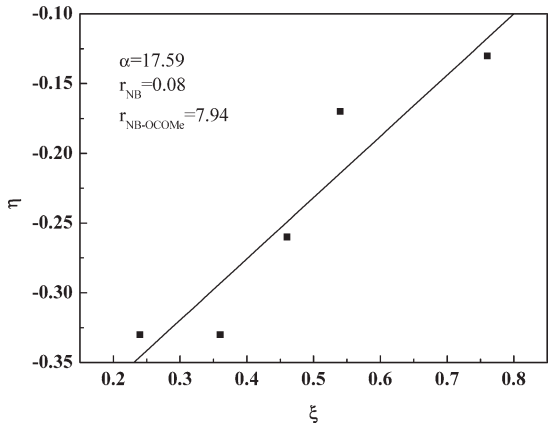

FIGURE 4 Linear fitting of the NB/NB-$OCOCH_3$ copolymerizations system catalyzed by Ni(II)/$B(C_6F_5)_3$ and according to Kelen–Tüdõs method.

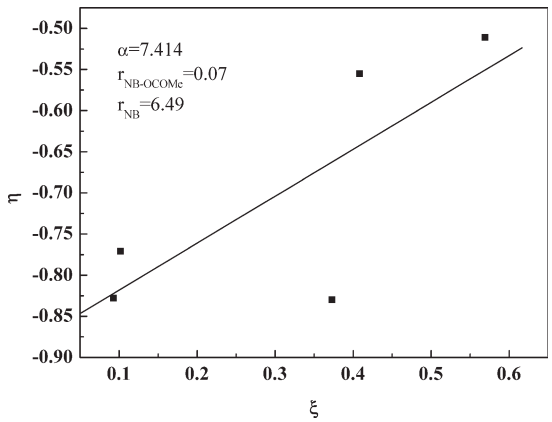

FIGURE 5 Linear fitting of the NB/NB-$OCOCH_3$ copolymerizations system catalyzed by Pd(II)/$B(C_6F_5)_3$ and according to Kelen–Tüdõs method.

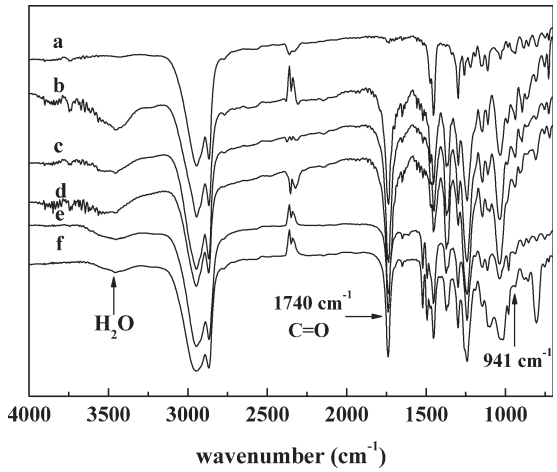

FIGURE 6 FTIR curves of NB/NB-$OCOCH_3$ copolymers with: (a) 0%, (b) 5.8%, (c) 10.3%, (d) 12.0%, (e) 3.5%, and (f) 3.7% of NBE-$OCOCH_3$ molar ratio. a, b, c, and d are obtained by Ni(II)/$B(C_6F_5)_3$. e and f are obtained by Pd(II)/$B(C_6F_5)_3$.

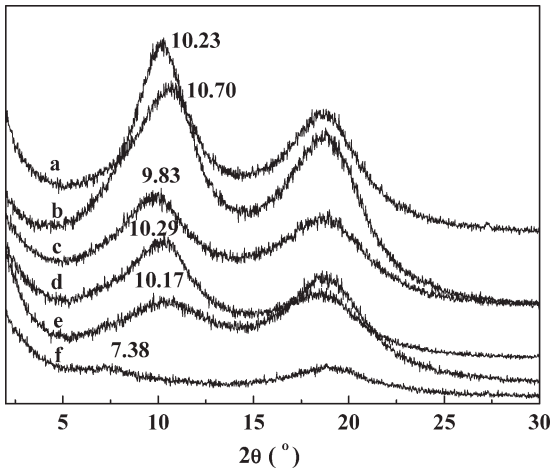

FIGURE 8 WXRD curves of NB/NB-$OCOCH_3$ copolymers with: (a) 0%, (b) 5.8%, (c) 10.3%, (d) 0%, (e) 3.5%, (d) 3.7%. a, b, and c are obtained by Ni(II)/$B(C_6F_5)_3$. d, e, and f are obtained by Pd(II)/$B(C_6F_5)_3$.

catalyzed to copolymerize by the complexes, a coordinated bond will be formed between metal atom and both of oxygen atoms and double-bond of NB-$OCOCH_3$ and NB.[48–50] The yields and the catalytic activities decreased obviously when the content of NB-$OCOCH_3$ increased in the comonomer feed ratio.

To obtain the reactivity ratios of the two monomers, we change the polymerization time and the feed content of catalysts to control the conversion rate to be under 10%. The results are shown in Table 4. The reactivity ratios are determined by the Kelen–Tüdõs method[51] (Figs. 4 and 5), which is shown in eqs 1–4.

$$x = [\mathrm{NB-OCOCH_3}]/[\mathrm{NB}];\ y = d[\mathrm{NB-OCOCH_3}]/d[\mathrm{NB}] \quad (1)$$

$$F = x^2/y;\ G = x(y-1)/y;\ \alpha = (F_{\max} \times F_{\min})^{0.5} \quad (2)$$

$$\eta = G/(\alpha + F);\ \xi = F/(\alpha + F) \quad (3)$$

$$\eta = (r_{\mathrm{NB-OCOCH3}} + r_{\mathrm{NB}}/\alpha)\xi - r_{\mathrm{NB}}/\alpha \quad (4)$$

For Ni(II)/$B(C_6F_5)_3$, the reactivity ratio of NB-$OCOCH_3$ is 0.08, and the reactivity ratio of NB is 7.94; For Pd(II)/$B(C_6F_5)_3$, the reactivity ratio of NB-$OCOCH_3$ is 0.07, and the reactivity ratio of NB is 6.49.

FTIR Spectra of Copolymers

The structures of copolymers were characterized by FTIR spectra and shown in Figure 6. The signal of double-bond at 1710 cm^{-1}, assigned to the C=C bond of the ROMP structure of PNB, was not observed. The signals at about 941 cm^{-1} could be attributed to the ring of bicyclo[2.2.1]heptanes further

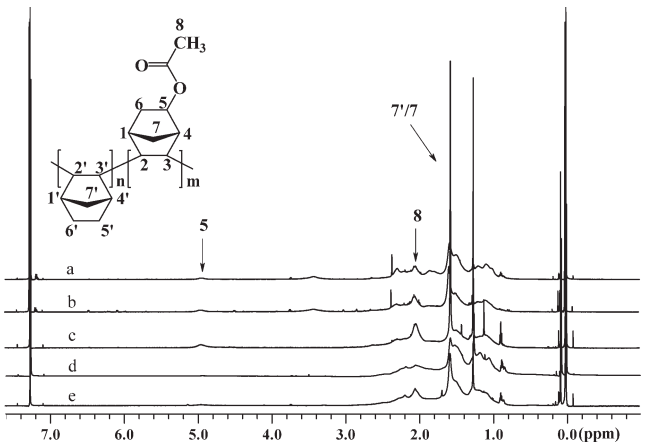

FIGURE 7 The ^1H NMR spectra of NB/NB-$OCOCH_3$ copolymers with: (a) 5.8%, (b) 10.3%, (c) 12.0%, (d) 3.5%, (e) 3.7% of NBE-$OCOCH_3$ molar ratio. a, b, and (c) obtained by Ni(II)/$B(C_6F_5)_3$, (d) and (e) obtained by Pd(II)/$B(C_6F_5)_3$.

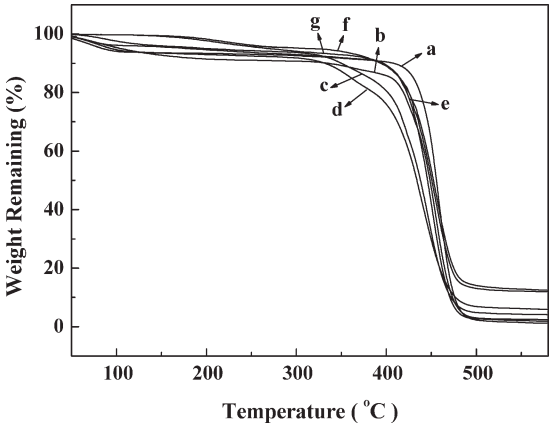

FIGURE 9 TGA curves of NB/NB-$OCOCH_3$ copolymers with: (a) 0%, (b) 5.8%, (c) 10.3%, (d) 12.0%, (e) 0%, (f) 3.5%, (g) 3.7% of NBE-$OCOCH_3$ molar ratio. a, b, c, and d are obtained by Ni(II)/$B(C_6F_5)_3$, and e, f, and g are obtained by Pd(II)/$B(C_6F_5)_3$. The T_d of the polymers are: (a) 421.1 °C, (b) 336.3 °C, (c) 323.7 °C, (d) 319.9 °C, (e) 400.0 °C, (f) 329.2 °C, (g) 317.5 °C.

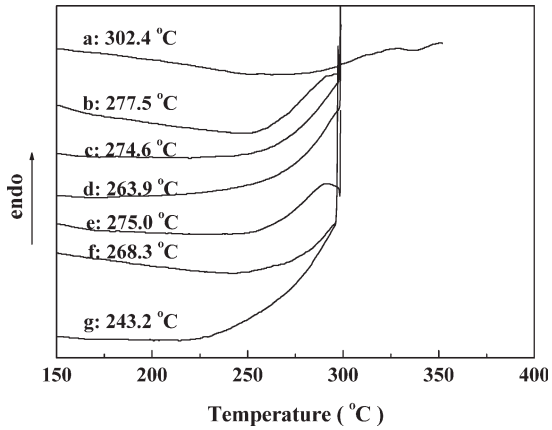

FIGURE 10 DSC curves of NB/NB-OCOCH$_3$ copolymers with: (a) 0%, (b) 5.8%, (c) 10.3%, (d) 12.0%, (e) 0%, (f) 3.5%, and (g) 3.7% of NBE-OCOCH$_3$ molar ratio. a, b, c, and d are obtained by Ni(II)/B(C_6F_5)$_3$, and e, f, and g are obtained by Pd(II)/B(C_6F_5)$_3$.

illustrating the monomers via vinyl-type addition polymerization. The observation at 1735 cm^{-1} in the spectra is the signal of C=O, and the signal became strong with increase of content of NB-OCOCH$_3$ and confirmed that the NB-OCOCH$_3$ has been inserted into the chains of the copolymers and to be true copolymer rather than blend polymer.

^{1}H NMR Spectra of Copolymers

The structures of the copolymers were also characterized by ^{1}H NMR spectra and shown in Figure 7. As shown in the ^{1}H NMR spectra, it proves that the polymers are vinyl-addition type by the absence of the resonance of the proton hydrogen connected to the double bond at 5.3–5.9 ppm. The peaks at 0.9–1.3 ppm can be assigned to the hydrogen corresponding to 5′/6′/6, the peaks at 1.5–1.7 ppm can be assigned to the hydrogen corresponding to 7′/7, the peaks at 1.9–2.2 ppm can be assigned to the hydrogen corresponding to 1′/2′/3′/4′/1/2/3/4/8, and the peaks at 5.0 ppm can be assigned to the hydrogen corresponding to 5. The content of NB-OCOCH$_3$

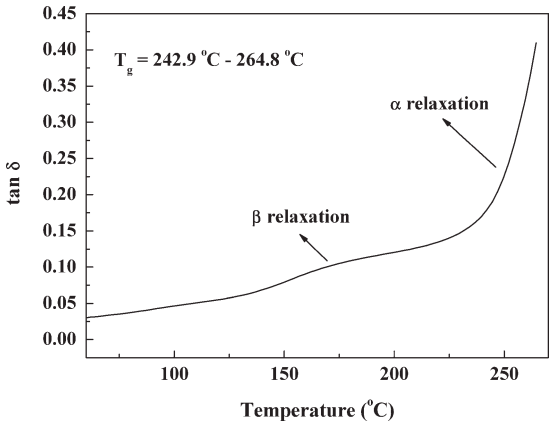

FIGURE 11 The loss modulus curves of NB/NB-OCOCH$_3$ copolymer films with 12.0% of NB-OCOCH$_3$ molar ratio and obtained by Ni(II)/B(C_6F_5)$_3$

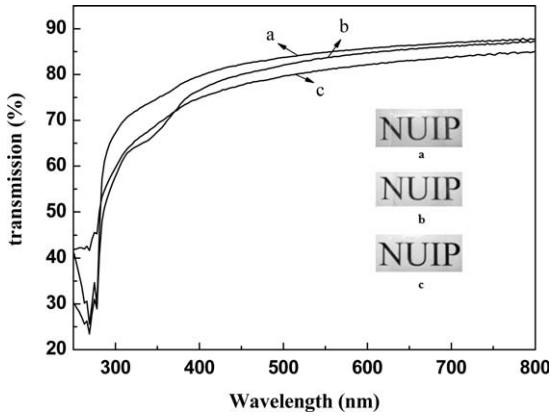

FIGURE 12 The UV–vis curves of NB/NB-OCOCH$_3$ copolymer films with: (a) 5.8%, (b) 10.3%, (c) 12.0% of NB-OCOCH$_3$ molar ratio and obtained by Ni(II)/B(C_6F_5)$_3$.

in copolymers can be calculated by the following eq 5,[39,40,52] and are (a) 5.8%, (b) 10.3%, (c) 12.0%, (d) 3.5%, (e) 3.7%.

$$\text{NB} - \text{OCOCH}_3\ \% = 2 \times I_{(5)}/I_{(7'/7)} \quad (5)$$

WXRD Analyses of the Copolymers

The WXRD curves of the copolymers with different NB-OCOCH$_3$ content prepared by Ni(II)/B(C_6F_5)$_3$ and Pd(II)/B(C_6F_5)$_3$ are shown in Figure 8. There is no trace of Bragg reflection in the characteristic of crystalline regions, so the polymers are noncrystalline. The peaking of the polymer whose content of NB-OCOCH$_3$ is 6.64% and changes little, but to other polymers, the intensity of both halos becomes weaker with the increase of NB-OCOCH$_3$ content. This result shows that NB-OCOCH$_3$ have insert into the polymer chain and further proved the obtained polymers are copolymer. Two broad halos at 2θ values of 7.38–10.70 and 18.54–18.89, which are characteristic for PNB were observed. The interchain distance is calculated according to eq 6[34] and are

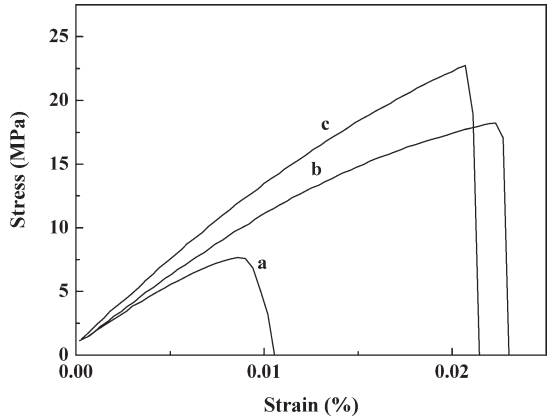

FIGURE 13 The tensile curves of NB/NB-OCOCH$_3$ copolymer films with: (a) 5.8%, (b) 10.3%, (c) 12.0% of NB-OCOCH$_3$ molar ratio and obtained by Ni(II)/B(C_6F_5)$_3$. The curves were recorded at a speed of 5 mm/min.

TABLE 5 The Mechanical Properties of NB/NB-$OCOCH_3$ Copolymer Films

Sample	Tensile Strength (MPa)	Elastic Modulus (GPa)	Elongation at Break (%)
a	7.7	1.04	4
b	18.2	1.11	3.4
c	22.7	1.32	3.7

Conditions: a, 5.8%; b, 10.3%; c, 12.0% of NB-$OCOCH_3$ molar ratio obtained by Ni(II)/B(C_6F_5)$_3$. The dates are recorded at a speed at 5 mm/min.

(a) 10.09 Å, (b) 10.55 Å, (c) 10.98 Å, (d) 10.49 Å, (e) 10.61 Å, and (f) 14.62 Å. The packing density became smaller with the increasing of NB-$OCOCH_3$ content in the copolymers, and the packing density of the copolymers obtained by Pd(II)/B(C_6F_5)$_3$ is smaller than those obtained by Ni(II)/B(C_6F_5)$_3$.

$$d_{\text{interchain}} = 1.22 d_{\text{Bragg}} = 1.22\lambda/(2\sin\theta) \quad (6)$$

TGA and DSC Analyses of Copolymers

The TGA curves of the copolymers with different NB-$OCOCH_3$ content prepared by Ni(II)/B(C_6F_5)$_3$ are shown in Figure 9. The decompose temperature (T_d) of the polymers are as high as 317.5–421.1 °C and decreases with NB-$OCOCH_3$ increased in copolymers. The T_d of the polymers obtained by Pd(II)/B(C_6F_5)$_3$ are lower than that of the polymers obtained by Ni(II)/B(C_6F_5)$_3$.

The DSC curves and glass transition temperature (T_g) of the copolymers with different NB-$OCOCH_3$ content prepared by Ni(II)/B(C_6F_5)$_3$ are shown in Figure 10. The T_g of the polymers are up to 243.2–302.4 °C when the content of NB-$OCOCH_3$ increased in the copolymers. The T_g of the polymers obtained by Pd(II)/B(C_6F_5)$_3$ are lower than the polymers obtained by Ni(II)/B(C_6F_5)$_3$.

The polymers with different NB-$OCOCH_3$ content prepared by Ni(II)/B(C_6F_5)$_3$ were dissolved in $CHCl_3$ and homopolymer of NB prepared by Ni(II)/B(C_6F_5)$_3$ and Pd(II)/B(C_6F_5)$_3$ were dissolved in *o*-dichlorobenzene as the mass fraction is 3%, after the solvent evaporated; the transparent polymer films were obtained. Unfortunately, the films of NB homopolymer cannot be obtained because of its brittle nature, and the copolymers prepared by Pd(II)/B(C_6F_5)$_3$ also cannot be obtained because of its low MW.

DMA Analyses of the Films

The DMA curves of the copolymer films with different NB-$OCOCH_3$ content were recorded by a TA Q800 DMA. The films became too brittle to break with the increase of the temperature and only the T_g of copolymer with 12.0% NB-$OCOCH_3$ content can be prepared. The loss factor curve of the copolymer with NB-$OCOCH_3$ content of 12.0% was shown in Figure 11. Following the insertion of NB-$OCOCH_3$, the β relaxation appeared due to the NB-$OCOCH_3$ group, and the T_g of copolymer in the α relaxation region can be also observed in the range of 242.9–264.8 °C. These results are consistent with that observed by DSC.

UV–Vis Spectra of the Films

The UV–vis curves of the copolymer films with different NB-$OCOCH_3$ content are shown in Figure 12. The films show high transmission in 400–800 nm and strong absorption in 250–400 nm. The copolymer film shows higher transmission with the NB-$OCOCH_3$ content decreased in the copolymers, the copolymer film, which contains 5.8% NB-$OCOCH_3$ shows highest transmission and up to 87.74%.

Mechanical Properties of the Films

The tensile curves of the copolymer films with different NB-$OCOCH_3$ content are shown in Figure 13, and the mechanical properties are presented in Table 5. As can be seen, the copolymer film shows better mechanical properties with the content of NB-$OCOCH_3$ increasing in the copolymers. The film of copolymer that contains 12.0% NB-$OCOCH_3$ shows best mechanical properties, the tensile strength is 22.7 MPa, the elastic modulus is 1.32 GPa. This phenomenon is due to the NB-$OCOCH_3$ can make the polymer chains flexible.

CONCLUSIONS

Two bis(β-ketoamino) type late transition metal complexes were synthesized, characterized by single crystal X-ray technique, and used for the copolymerization of NB and NB-$OCOCH_3$ together with B(C_6F_5)$_3$. The catalytic activities of two complexes on homopolymerization of NB are as high as 10^5 $g_{polymer}/mol_{Mt}$ h. Toward the copolymerization of NB and NB-$OCOCH_3$, Ni (II)/B(C_6F_5)$_3$ shows high activity, whereas Pd(II)/B(C_6F_5)$_3$ shows very lower activity and the catalytic activities decreased with increasing of NB-$OCOCH_3$ in feed content. The reactivity ratios were determined to be $r_{\text{NB-OCOMe}} = 0.08$, $r_{\text{NB}} = 7.94$ for Ni(II)/B(C_6F_5)$_3$; and $r_{\text{NB-OCOMe}} = 0.07$, $r_{\text{NB}} = 6.49$ for Pd(II)/B(C_6F_5)$_3$ by Kelen–Tüdõs method. The structures of the obtained polymers are confirmed to be vinyl-addition polymer by ^{1}H NMR and FTIR characterizations. The copolymers of NB and NB-$OCOCH_3$ exhibited better solubility and mechanical properties than that of NB homopolymer and show high transparency and high glass transition temperature (T_g = 263.9–277.5 °C). With the increase of NB-$OCOCH_3$ content, the MW, T_g, and T_d decreased, whereas the mechanical properties became better and the packing density became smaller. When compared with the copolymers obtained by Ni(II)/B(C_6F_5)$_3$, copolymer obtained by Pd (II)/B(C_6F_5)$_3$ shows relative lower T_g, T_d, MW, and packing density.

Financial support for this work was provided by the National Natural Science Foundation of China (51073076, 50902067, and 51003045).

REFERENCES AND NOTES

1 Kennedy, J. P.; Makowski, H. S. J Macromol Sci A 1967, 1, 345–370.

2 Gaylord, N. G.; Deshpande, A. B.; Mandal, B. M.; Martan, M. J Macromol Sci A 1977, 11, 1053–1070.

3 Myagmarsuren, G.; Lee, K.-S.; Jeong, O.-Y.; Ihm, S.-K. Catal Commun 2003, 4, 615–619.

4 South, C. R.; Leung, K. C. F.; Lanari, D.; Stoddart, J. F.; Weck, M. Macromolecules 2006, 39, 3738–3744.

5 Quémener, D.; Bousquet, A.; Héroguez, V.; Gnanou, Y. Macromolecules 2006, 39, 5589–5591.

6 Nair, K. P.; Weck, M. Macromolecules 2007, 40, 211–219.

7 Mathers, R. T.; Damodaran, K.; Rendos, M. G.; Lavrich, M. S. Macromolecules 2009, 42, 1512–1518.

8 Li, Z.; Ma, J.; Cheng, C.; Zhang, K.; Wooley, K. L. Macromolecules 2010, 43, 1182–1184.

9 Weck, M.; Schwab, P.; Grubbs, R. H. Macromolecules 1996, 29, 1789–1793.

10 Silva Sá, J. L.; Vieira, L. H.; Nascimento, E. S. P.; Lima-Neto, B. S. Appl Catal A: General 2010, 374, 194–200.

11 Silva Sá, J. L.; Lima-Neto, B. S. J Mol Catal A: Chemical 2009, 304, 187–190.

12 Nishizawa, O.; Misaka, H.; Kakuchi, T.; Satoh, T. J Polym Sci Part A: Polym Chem 2008, 46, 1185–1191.

13 Hu, T.; Li, Y.-G.; Li, Y.-S.; Hu, N.-H. J Mol Catal A: Chem 2006, 253, 155–164.

14 Chen, J.-X.; Huang, Y.-B.; Li, Z.-S.; Zhang, Z.-C.; Wei, C.-X.; Lan, T.-Y.; Zhang, W.-J. J Mol Catal A: Chem 2006, 259, 133–141.

15 Bao, F.; Lü, X.-Q.; Gao, H.-Y.; Gui, G.-Q.; Wu, Q. J Polym Sci Part A: Polym Chem 2005, 43, 5535–5544.

16 Tarte, N. H.; Woo, S. I.; Cui, L.-Q.; Gong, Y.-D.; Hwang, Y. H. J Organometallic Chem 2008, 693, 729–736.

17 Myagmarsuren, G.; Park, J.-I.; Ihm, S.-K. Polymer 2006, 47, 8474–8479.

18 Liang, H.; Liu, J.-Y.; Li, X.-F.; Li, Y.-S. Polyhedron 2004, 23, 1619–1627.

19 Barnes, D. A.; Benedikt, G. M.; Goodall, B. L.; Huang, S. S.; Kalamarides, H. A.; Lenhard, S.; McIntosh, L. H., III; Selvy, K. T.; Shick, R. A.; Rhodes, L. F. Macromolecules 2003, 36, 2623–2632.

20 Long, J.-M.; Gao, H.-Y.; Liu, F.-S.; Song, K.-M.; Hu, H.; Zhang, L.; Zhu, F.-M.; Wu, Q. Inorg Chim Acta 2009, 362, 3035–3042.

21 Lassahn, P.-G.; Janiak, C.; Oh, J.-S. Macromol Rapid Commun 2002, 23, 16–20.

22 Terao, H.; Iwashita, A.; Ishii, S.; Tanaka, H.; Yoshida, Y.; Mitani, M.; Fujita, T. Macromolecules 2009, 42, 4359–4361.

23 Li, Y.-F.; Gao, H.-Y.; Wu, Q. J Polym Sci Part A: Polym Chem 2008, 46, 93–101.

24 He, L.-P.; Liu, J.-Y.; Li, Y.-G.; Liu, S.-R.; Li, Y.-S. Macromolecules 2009, 42, 8566–8570.

25 Sudhakar, P. J Polym Sci Part A: Polym Chem 2008, 46, 444–452.

26 Ravasio, A.; Zampa, C.; Boggioni, L.; Tritto, I.; Hitzbleck, J.; Okuda, J. Macromolecules 2008, 41, 9565–9569.

27 Woodman, T. J.; Sarazin, Y.; Garratt, S.; Fink, G.; Bochmann, M. J Mol Catal A: Chem 2005, 235, 88–97.

28 Leone, G.; Boglia, A.; Boccia, A. C.; Scafati, S. T.; Bertini, F.; Ricci, G. Macromolecules 2009, 42, 9231–9237.

29 Kaminsky, W.; Derlin, S.; Hoff, M. Polymer 2007, 48, 7271–7278.

30 Cai, Z.-G.; Nakayama, Y.; Shiono, T. Macromolecules 2006, 39, 2031–2033.

31 Cai, Z.-G.; Harada, R.; Nakayama, Y.; Shiono, T. Macromolecules 2010, 43, 4527–4531.

32 Shiono, T.; Sugimoto, M.; Hasan, T.; Cai, Z.-G.; Ikeda, T. Macromolecules 2008, 41, 8292–8294.

33 Hou, Z.-M.; Luo, Y.-J.; Li, X.-F. J Organometallic Chem 2006, 691, 3114–3121.

34 Mi, X.; Ma, Z.; Wang, L.-Y.; Ke, Y.-C.; Hu, Y.-L. Macromol Chem Phys 2003, 204, 868–876.

35 Kim, I.; Hwang, J.-M.; Lee, J. K.; Ha, C. S.; Woo, S. I. Macromol Rapid Commun 2003, 24, 508–511.

36 Kaita, S.; Matsushita, K.; Tobita, M.; Maruyama, Y.; Wakatsuki, Y. Macromol Rapid Commun 2006, 27, 1752–1756.

37 Ogata, K.; Watanabe, A.; Yunokuchi, T.; Toyota, A. Inorg Chem Commun 2008, 11, 215–219.

38 Shin, D. M.; Son, S. U.; Hong, B. K.; Chung, Y. K.; Chun, S.-H. J Mol Catal A: Chem 2004, 210, 35–46.

39 Wang, L.-Y.; Li, Y.-F.; Zhu, F.-M.; Wu, Q. Euro Polym J 2006, 42, 322–327.

40 He, F.-P.; Chen, Y.-W.; He, X.-H.; Chen, M.-Q.; Zhou, W.-H.; Wu, Q. J Polym Sci Part A: Polym Chem 2009, 47, 3990–4000.

41 Wang, B.-L.; Tang, T.; Li, Y.-S.; Cui, D.-M. Dalton Trans 2009, 8963–8969.

42 He, X.-H.; Yao, Y.-Z.; Luo, X.; Zhang, J.-K.; Liu, Y.-H.; Zhang, L.; Wu, Q. Organometallics 2003, 22, 4952–4957.

43 Gao, H.-Y.; Liu, X.-F.; Pei, L.-X.; Wu, Q. J Polym Sci Part A: Polym Chem 2009, 48, 1113–1121.

44 Walter, M. D.; Moorhouse, R. A.; White, P. S.; Brookhart, M. J Polym Sci Part A: Polym Chem 2009, 47, 2560–2573.

45 Vougioukalakis, G. C.; Stamatopoulos, I.; Petzetakis, N.; Raptopoulou, C. P.; Psycharis, V.; Terzis, A.; Kyritsis, P.; Pitsikalis, M.; Hadjichristidis, N. J Polym Sci Part A: Polym Chem 2009, 47, 5241–5250.

46 O'Connor, A. R.; Brookhart, M. J Polym Sci Part A: Polym Chem 2010, 48, 1901–1912.

47 Morishita, H.; Sudo, A.; Endo, T. J Polym Sci Part A: Polym Chem 2009, 47, 3982–3989.

48 Casares, J. A.; Espinet, P.; Salas, G. Organometallics 2008, 27, 3761–3769.

49 Wendt, R. A.; Angermund, K.; Jensen, V.; Thiel, W.; Fink, G. Macromol Chem Phys 2004, 205, 308–318.

50 Funk, J. K.; Andes, C. E.; Sen, A. Organometallics 2004, 23, 1680–1683.

51 Kelen, T.; Tüdõs, F. J Macromol Sci A 1975, 9, 1–27.

52 Peruch, F.; Cramail, H.; Deffieux, A. Macromol Chem Phys 1998, 199, 2221–2227.